

The ACE Genes in *Aphelenchoides besseyi* Isolates and Their Expression Correlation to the Fenamiphos Treatment

Jung-Kai Hsu

National Chung Hsing University

Chia-Wei Weng

Chung Shan Medical University

Jeremy J.W. Chen

National Chung Hsing University

Peichen J. Chen (✉ janetchen@nchu.edu.tw)

National Chung Hsing University

Research Article

Keywords: *Aphelenchoides besseyi*, acetylcholinesterase, AChE-inhibitors insensitivity

Posted Date: June 1st, 2021

DOI: <https://doi.org/10.21203/rs.3.rs-566994/v1>

License:  This work is licensed under a Creative Commons Attribution 4.0 International License.

[Read Full License](#)

Version of Record: A version of this preprint was published at Scientific Reports on February 7th, 2022.

See the published version at <https://doi.org/10.1038/s41598-022-05998-y>.

Abstract

Aphelenchoides besseyi could cause great yield loss on rice and many economically important crops. Acetylcholinesterase inhibitors were commonly used to mitigate plant parasitic nematodes. However, increasing nematicide-resistance has been reported due to the extensive use of these chemicals. The correlation between the AChE-inhibitor (fenamiphos) sensitivities and acetylcholinesterase (*ace*) genes in two isolates of *A. besseyi* (designated RI and HSF) was established. The LD₅₀ of fenamiphos to RI and HSF were 572.2 ppm and 129.4 ppm, respectively, indicating that two nematode isolates had different sensitivities to fenamiphos. Three *ace* genes were cloned and sequenced in *A. besseyi*, and their homology was supported by phylogenetic analysis with AChEs protein sequences from various vertebrate and invertebrate species. Molecular docking showed that the affinities of each AChEs to fenamiphos were higher in HSF isolate, indicating that there should be point mutations in RI isolate AChEs. Treating the two isolates with 100 ppm fenamiphos for 12 h, three *ace* genes of HSF isolate were down-regulated but were up-regulated in RI isolate. The results suggest that fenamiphos can transcriptionally modulate the expression of *ace* genes, as well as the variants in AChEs and increased expression of *ace* genes might be associated with fenamiphos-insensitivity in RI isolate.

Introduction

Plant parasitic nematodes were estimated to cause \$US16 billion rice yield loss annually¹. Rice white tip nematodes, *Aphelenchoides besseyi* could be responsible for 10–30% of the total damage to rice crops, and up to 70% yield loss on highly susceptible rice variety^{2,3}. *A. besseyi* had not only been found on rice, but also other economical crops including strawberry, chrysanthemum, and bird's-nest fern. *A. besseyi* is difficult to control as it has a wide host range and could feed on fungi^{4–6}.

Soaking rice seeds with nematicides is the most common strategy for controlling *A. besseyi*. Nematicides including organophosphates (OPs) and carbamates (CBs) that act by inhibiting acetylcholinesterase (AChE, EC 3.1.1.7) are widely recommended for this purpose. Those nematicides are widely used in agricultural pest managements because of their high efficacy and low cost⁷. Inhibition of acetylcholinesterase by AChE-inhibitors leads to the accumulation of acetylcholine, which is an important neurotransmitter in many types of animals, thereby causing mortality in nematodes^{8,9}. However, a low nematode mortality rate has been observed in rice seeds even after being soaked with nematicide, likely due to the protection of glumes or nematicide-resistance in nematodes¹⁰. Pesticides resistance has been a concerning issue since mid-1940s because of the extensive and repeated use of these chemical agents^{11,12}. Although the mode of action of OPs and CBs insecticides has been intensively studied in insects, little is known about the mechanisms by which plant-parasitic nematodes confer resistance to AChE-inhibitors.

Target site insensitivity is one of the most common mechanisms leading to pesticide resistance, which could cause the difficulty in pest management^{12–15}. Point mutations in various positions of AChE of

insects have been reported to result in resistance to AChE inhibitor insecticides¹⁵. Organophosphate and carbamate insecticides are used to control *Anopheles* spp., the major mosquito vectors of malaria. The resistance of the mosquito to both these insecticides has been found to be resulted from a point mutation in AChE1 (G119S), which led to a reduced susceptibility to most AChE-inhibitors^{16–18}. Animal parasitic nematode *Haemonchus contortus* displaying resistance to benzimidazoles has also been proved to be the result of point mutations on the target site protein β-tubulin (F200Y with F167Y or E198A)¹⁹. The plant-parasitic nematode, *M. incognita* has been reported that 18 point mutations in AChE2 are associated with the fosthiazate resistance²⁰.

In addition to target site insensitivity, overexpression of neuronal AChE and production of non-neuronal AChE are involved in resistance to AChE-inhibitors²¹. Overexpression of neuronal AChE could be due to transcriptional activation and duplication of the *ace* genes. As the amount of AChE increases, the pests could become more resistant to AChE-inhibitors²². For instance, up-regulation of a single copy of the *ace* gene in *Drosophila* sp. has been shown to lead to parathion resistance²³. Similar phenomena have also been found in organophosphate-resistant greenbug (*Schizaphis graminum*)²⁴. Duplication of the *Ace* genes has been found in some cases of insecticide-resistance often resulting in higher AChE catalytic efficiency and resistance to AChE-inhibitors^{21,25,26}. Non-neuronal AChE can affect cellular sensitivity to AChE-inhibitors by interfering the function of AChE-inhibitors²¹. In a study involving mammalian cells, cells become more resistant to organophosphate as the result of the non-neuronal soluble read-through AChE (AChE-R), which could repair neurodegeneration and avoid cell damage upon exposure to organophosphate²⁷. Studies have also found that both *Caenorhabditis elegans* and *Bursaphelenchus xylophilus* nematodes have a non-neuronal AChE3 gene, which has been shown to be responsible for xenobiotic substances defensing^{28–30}

Two *A. besseyi* isolates designated R1 and HSF were isolated from rice and bird-nest fern, respectively. Sensitivity tests to fenamiphos, an AChE-inhibitor nematicide revealed a drastic difference between these two isolates, in which the R1 isolate was highly tolerant and the HSF isolate was sensitive to fenamiphos. The objective of this study was to determine whether *A. besseyi* confers resistance to AChE-inhibitors is resulted from mutations of the acetylcholinesterase-coding gene (*ace*). The *ace* genes of *A. besseyi* R1 and HSF isolates were identified and sequenced. The 3D-structures of AChEs were revealed based on computational predictions. Molecular docking analysis of these AChEs was performed to predict whether mutations in AChE were responsible for the fenamiphos insensitivity. qRT-PCR was applied to determine the expression levels of the *ace* genes in R1 and HSF isolates before and after fenamiphos treatment.

Methods

Collection and identification of Nematodes

Aphelenchoides besseyi R1 isolate was collected from rice leaves in Linnei township, Yunlin County, and the HSF isolate was collected from bird's nest ferns in Huisun experimental forest, Nantou County. No

approvals were required for the study, which complied with all relevant ethical parameters for plant usage. These two isolates were established by single female according to Jen *et al.*³¹. The RI and HSF isolates were identified to species according to the morphological characters and the 18S rRNA sequences³². Nematodes were reared on *Alternaria citri* slant at 27°C.

The nematicide bioassays

Fenamiphos (Merck, Darmstadt, Germany, #45483-250MG), an organophosphate nematicide, was dissolved in acetone for the following treatments. The nematicide bioassay was modified from the protocol described by Kang *et al.*⁷. Fenamiphos was diluted to five stock concentrations: 5000, 10000, 20000, 30000 and 50000 ppm. Nematodes were washed out from a slant using 2-ml ddH₂O. Nematode suspensions (495 µl) containing approximately 150 nematodes were mixed with 5 µl stock fenamiphos in a 1.5 ml microcentrifuge tube. The final treating concentrations were 50, 100, 200, 300, 500 ppm, respectively. The nematodes treated with fenamiphos were incubated at 27°C for 24 h on a shaker in the dark, and the mortality rates were recorded. Nematodes that were rigidity and after touching remained motionless for 3 seconds after touching were presumed dead. Each treatment had three replicates, and the experiment was repeated three times. The data was plotted as dose-response curves.

The mortality progress curve of these 2 isolates was obtained as follows. Two nematode isolates were treated with the highest concentration of fenamiphos and the mortality rates were hourly recorded for 12 h and the last data was taken at 24 h post-treatment. Each isolate had three replicates and the experiment was repeated three times.

The dose-response regression curves with standard error and the median lethal doses (LD₅₀) were deduced by the 'drc' package³³ in R environment. Dose-response regression curves and mortality progress curves were plotted by 'ggplot2' package.

RNA and cDNA preparation

All stages of *A. besseyi* were washed with sterile distilled water from the *A. citri* slant and purified by the modified Bearmann funnel technique for 12 h before total RNA extraction. For qRT-PCR, nematodes mixed with 100 ppm fenamiphos were incubated at 27°C for 12 h on placed on a shaker in the dark. After treatment, nematodes were washed two times with ddH₂O before RNA extraction. GENEzol™ TriRNA Pure Kit (Geneaid, New Taipei City, Taiwan) was used to extract total RNA according to the manufacturer's instructions. Single stranded cDNA was synthesized using SuperScript III Reverse Transcriptase (Invitrogen, California, USA), using an oligo-dT primer.

Identification of *A. besseyi* acetylcholinesterase (ace) genes

Sequences including the *Bursaphelenchus xylophilus* ace genes (Accession Nos: ACZ64207.1, ACZ64208.1, ACZ64209.1) and the *Ditylenchus destructor* ace genes (Accession Nos: ABQ58117.1, ABQ58116.1, ABQ58115.1) were used as templates to blast *A. besseyi* transcriptome database (Accession: SRX385206) to identify the reserved regions of the gene. The primers (Table S1) used for the

following experiments were designed based on the conserved regions. The 3' and 5' cDNA ends flanking the acetylcholinesterase coding gene were obtained by 3' RACE and 5' RACE System for the Rapid Amplification of cDNA Ends (Invitrogen, Carlsbad, California, USA, #18373-019 and #18374-058). The RACE PCR was first performed followed by a nest PCR in the same tube. The PCR started with denaturation at 94°C for 3 min, followed by 35 cycles of 94°C for 45 s, 58°C for 45 s, and 72°C for 1 min 30 s, and a final extension at 72°C for 10 min. The PCR products were separated in 1.2% agarose gels and stained with 40 ppm ethidium bromide solution. Target gene products were recovered from the gel with the Gel Elution Kit (GeneMark, Taipei, Taiwan, #DP03) and cloned into a vector with the TOPO TA Cloning kit (Invitrogen, Carlsbad, California, USA). Plasmids were propagated in *Escherichia coli* DH5α cells, extracted and sent to the NCHU Biotechnology Center (Taichung, Taiwan) for sequencing. Each *ace* gene of two *A. besseyi* isolates were sequenced from three biological repeats, and three independent clones with target gene were used for sequencing in each repeat.

Bioinformatics analysis of ace genes

Open Reading Frame Finder (ORF Finder, <https://www.ncbi.nlm.nih.gov/orffinder/>) was used to locate the start codon and stop codon of *ace* genes. The ORF sequences of *ace* genes were translated into Acetylcholinesterase (AChE) protein sequences and used for phylogenetic analysis and prediction of protein functional domains. Protein sequences of AChEs from other vertebrates, nematodes and arthropods used in the phylogenetic analysis³⁴ were downloaded from NCBI database. Multiple alignment analysis was performed by ClustalW with default parameters. The phylogenetic tree was conducted using the Maximum Likelihood method with LG model and Gamma Distributed (G) with 500 bootstrap replicates³⁵⁻³⁷.

Protein sequences of AChEs were aligned with AChEs from *Torpedo californica*, *Homo sapiens*, and *Drosophila melanogaster* (SwissProt codes: ACES_TETCF, ACES_HUMAN and ACES_DROME). The functional domains were located based on the reported AChE³⁸. Transmembrane domains, signal peptides and Glycosylphosphatidylinositol (GPI) Anchors were predicted by TMHMM Server v. 2.0, SignalP-5.0 Server and PredGPI GPI-Anchor Predictor, respectively³⁹⁻⁴².

Molecular docking evaluation

The 3D structures of three AChE proteins obtained from *A. besseyi* HSF and RI isolates were homology-modeled by using the I-TASSER standalone package version 5.1⁴³ with default parameters. The simulated structures were applied in the molecular docking study using the Discovery Studio software (BIOVIA, San Diego, CA, USA)⁴⁴ to assess the probably binding modes of fenamiphos in AChE active site. The initial structures were prepared using the Prepare Protein protocol in Discovery Studio to insert missing loop regions based on SEQRES data and to protonate the structures at pH 7.4. The crystal structure of *Torpedo californica* AChE in complex with acetylcholine (PDB code: 2ACE)⁴⁵ was employed as reference structure to determine the docking site through the superimposition of the simulated structures onto the co-crystallized structure. The docking was performed using the CDOCKER⁴⁶ docking

protocol in Discovery Studio and potentials were added applying the CHARMM force field⁴⁷. Conformations of fenamiphos were generated via random rotations and high-temperature molecular dynamics, and then were refined by grid-based simulated annealing and minimization. The best docking poses were selected following the highest docking energy scores. The post-docking analyses were performed using the LigPlot + software⁴⁸ to identify the ligand-protein hydrogen bonds and hydrophobic moieties.

Quantitative RT-PCR (qRT-PCR)

qRT-PCR was used to assess the expression levels of the *ace* genes in two different *A. besseyi* isolates treated with or without 100 ppm fenamiphos. CFX Connect Real-Time PCR Detection System (Bio-Rad Laboratories, Inc) was used to conduct gene expression analysis. The specific primers of one 18 small-subunit ribosomal (18S) gene and three *ace* genes were designed (Table S1) to detect gene expression levels and the 18s gene was used as the internal reference gene in the experiment. For each primer pair, PCR efficiencies were determined by standard curves. The qRT-PCR conditions were set as follow: 95°C for 3 min, 40 cycles of 95°C for 10 s and 59.5°C for 30 s, following a dissociation stage. Efficiencies of primer pairs in RI isolate are 83.5% (18S), 96.4% (*ace1*), 96.6% (*ace2*), and 99.3% (*ace3*). In HSF isolate, efficiencies of primer pairs are 83.7% (18S), 92.2% (*ace1*), 95.5% (*ace2*), and 90.3% (*ace3*) (all with $R^2 \geq 0.999$). Concentrations of each cDNA were adjusted to about 1 ng/ μ l. qRT-PCR of four genes (18S, *ace1*, *ace2* and *ace3*) from two nematode isolates were conducted with three technical replicates and three biological replicates. Data were analyzed with the $\Delta\Delta CT$ method and compared between untreated and fenamiphos-treated groups by one-tailed Student's *t*-test. Data after analyzing by the $\Delta\Delta CT$ method were converted to fold changes, and plotted in R environment by 'ggplot2' package.

Results

Confirming nematode species

Both RI and HSF isolates had morphological characteristics resembling *Aphelenchoides*. Both isolates had offset lip region. The metacorpus width is larger than 75% body width, pharyngeal glands overlapping ventrally and 3–4 mucros at the tail tip⁴⁹. The 18S rRNA sequences of the RI and HSF isolates had 100% and 99.56% identity to *Aphelenchoides besseyi* (#KT454963 and #KT454962), respectively, and both had zero E value. HSF and RI isolates used in this study were identified as *Aphelenchoides besseyi* based on sequence similarity and morphological characteristics.

The AChE inhibitor sensitivity of two *A. besseyi* isolates

In the fenamiphos bioassay, the results indicated that the median lethal dose (LD_{50}) of RI and HSF isolates to fenamiphos was 129.367 ppm and 572.236 ppm, respectively. The dose-response regression curves showed that RI isolate was less sensitive to fenamiphos than HSF isolate (Fig. 1). The mortality progress curves showed that these two isolates had different responses to 500 ppm fenamiphos in the

first 12 h post-treatment (Fig. 2). The curve of HSF isolate showed a larger slope compared to that of RI isolate, indicating further that RI isolate was less sensitive to fenamiphos.

Three acetylcholinesterase genes in *A. besseyi*

Both HSF and RI isolates have three *ace* genes, designated *Abeace1-RI*, *Abeace1-HSF*, *Abeace2-RI*, *Abeace2-HSF* *Abeace3-RI* and *Abeace3-HSF*. Sequences of three genes were submitted to the Genebank database (accession no. MT431320- MT431325). Based on sequence analysis, open reading frames of *Abeace1-RI*, *Abeace2-RI* and *Abeace3-RI* were 1884 bp, 1908 bp and 1815 bp, respectively. *Abeace1-HSF*, *Abeace2-HSF* and *Abeace3-HSF* had an ORF of 1887 bp, 1914 bp and 1815 bp, respectively. The proteins encoded by the *ace* genes were named AChE1, AChE2 and AChE3. Amino acid sequences of six *ace* genes were aligned with 3 BuChEs from vertebrates and 37 AChEs from vertebrates, arthropods and nematodes, and their phylogenetic relationships with an esterase amino acid sequence from *Caenorhabditis elegans* as an outgroup was analyzed. The phylogeny tree indicated that each of AChE1, AChE2 and AChE3 from *A. besseyi* was independently grouped with AChE1, AChE2 and AChE3 of plant-parasitic nematodes (Fig. 3). Phylogenetic analysis indicated that AChE1 of both *A. besseyi* isolates was most similar to arthropods AChE1, followed by vertebrates AChE and BuChE. Meanwhile, AChE2/3 of both *A. besseyi* isolates were grouped independently in the same clade with AChE2/3/4 of other nematodes.

Predicting functional domains of AbeAChEs from two *A. besseyi* isolates

A. besseyi AChEs contained six functional domains resembling those found in the *Torpedo californica* AChE (TcAChE) (Fig. 4). Sequence alignment showed that amino acid differences between three AbAChEs were found in the choline-binding site, the Acyl pocket, the peripheral site and the flexible peripheral site loop. However, no ambiguities were found in AChEs between two nematode isolates. No substitution was found at catalytic residues in catalytic triad or oxyanion hole between AbeAChEs and TcAChE. The alignment also revealed three AbeAChEs might pose different binding abilities due to the differences in their choline-binding site and peripheral sites. AChE1/2 had signal peptides and transmembrane domains at N-terminus. AChE3 had transmembrane domains at C-terminus and only AChE2 had GPI-anchors at C-terminus.

Molecular docking

A molecular modeling study was performed to estimate the binding affinity of fenamiphos in acetylcholine-binding pocket of the simulated 3D structures of three AChE proteins obtained from *A. besseyi* HSF and RI isolates. The docking energy scores for the AChE1 and AChE3 proteins in HSF isolate (Docking score of AChE1: -26.79 kcal/mol; Docking score of AChE3: -19.33 kcal/mol) were significantly higher than that for the RI isolate (Docking score of AChE1: -2.84 kcal/mol; Docking score of AChE3: -5.43 kcal/mol). The docking analysis of AChE2 protein also revealed a slight difference of docking energy scores between HSF isolate (-22.74 kcal/mol) and R1 isolate (-21.51 kcal/mol). Further post-docking analyses indicated that several equivalenced residues surrounding the binding pocket of individual AChE

proteins in both HSF and RI isolates were predicted to form the hydrogen bonds and hydrophobic interactions (Fig. 5). Among these interactions, the hydrophobic interactions between fenamiphos and AChE1 protein were found on Trp102, Tyr354, and Phe355 in the AChE1 of HSF isolate and Tyr353 and Phe354 in the AChE1 of RI isolate. Those amino acids are required for binding to choline. However, the hydrogen bond interactions were found on Gly138 and Trp101 of the AChE1 proteins in HSF isolate and RI isolate, respectively. The hydrophobic interactions within choline-binding site on AChE2 protein were found on Trp115, Tyr367, and Trp368 in HSF isolate and Trp113, Tyr365, and Trp366 in RI isolate. Two regulatory residues (Trp109 and Trp356) in HSF isolate and three regulatory residues (Trp109, Phe355, and Trp356) in RI isolate were also identified to form the hydrophobic moieties on choline-binding site of the AChE3 protein (Fig. 5). Furthermore, the hydrogen bond was only found on His469 residue in HSF isolate to produce more steady interaction than RI isolate. The results suggested that three AChE proteins of HSF isolate have a higher binding affinity for fenamiphos than those of RI isolate due to the difference in hydrogen bond force field, especially for AChE1 and AChE3 proteins.

Ace genes were up-regulated after fenamiphos-treating in RI isolate

The transcript abundance of three *ace* genes were quantified by qRT-PCR. The basal expression levels of *ace* genes of untreated HSF and RI isolates were obtained. HSF showed higher expression levels of *ace1*, *ace2*, and *ace3*, which were 274.0fold, 2.6-fold and 3.5-fold higher than those of RI *ace* genes, respectively. In the individuals, *ace2* presented the highest expression level, followed by *ace3* and *ace1* in both RI and HSF isolates (Fig. 6).

Three *ace* genes in the fenamiphos sensitive HSF isolate were significantly down-regulated after fenamiphos treatment. Among them, *ace1* was 0.0008-fold decrease($P= 0.00095$), *ace2* was 0.203-fold decrease($P= 0.005$) and *ace3* was 0.095-fold decrease($P= 0.00093$) compared to the untreated ones (Fig. 7a-c). However, in RI isolate, significant up-regulation of *ace* genes was detected after fenamiphos treatment, the expression levels of *ace1*, *ace2*, and *ace3* of the treated RI isolate were 121.937-fold($P= 0.0085$), 2.255-fold($P= 0.05$), and 2.473-fold($P= 0.01$) higher than those in the untreated nematodes, respectively (Fig. 7a-c).

Discussion

In rice cultivation systems, fenamiphos is one of the main nematicides recommended for controlling seed-borne rice white-tip nematode (*Aphelenchoides besseyi*). In Taiwan, fenamiphos is recommended to be applied by pre-soaking rice seeds in water for 24 h then followed by soaking in 400 ppm fenamiphos for 2 h. However, the soaking application fails to effectively reduce rice white-tip nematode incidences^{3,10}. Our data indicated that *A. besseyi* originated from different hosts were observed to have different fenamiphos susceptibilities. The LD₅₀ of the rice-originated RI isolate to fenamiphos was 572.2 ppm, which was 4.4 time greater than that of the fern-originated HSF isolate which was collected from a site that has not been exposed to pesticides. It appears that RI isolate has lower sensitivity to fenamiphos than HSF. The mortality progress curve showed that the insensitive RI isolate after being treated by 500

ppm of fenamiphos for 2 h, had lower than 25% mortality. This indicates that the currently recommended dosage and 2-hour-treatment for rice seeds might not be able to eradicate the survival stages of *A. besseyi* in the rice seeds. Either higher dosage or longer nematicide-soaking time should be recommended for rice seeds sanitizing.

Nematicides resistance is an intricate phenomenon in which multiple mechanisms are involved^{19,50}; but mounting evidence has showed that the nematicides mainly target acetylcholinesterase genes^{21,38} are one of the major reason. In this study, three *ace* genes in *A. besseyi* were first sequenced and reported. We have found that *Abeace-1*, *Abeace-2* and *Abeace-3* are orthologous with *ace* genes from other nematodes. Nematode AChE1 is closer to arthropod AChE1, followed by vertebrate AChE and BuChE (Fig. 3). Nematode AChE2/3/4 proteins are independently grouped to different clades. In the evolution of AChE, the duplication event of *ace* loci likely leads to multiple *ace* genes in nematode during the period of divergence of Protostomia, and nematode AChE2/3/4 have more ancient evolutionary origins than nematode AChE1, which shares the ancestor with arthropod AChE1 and vertebrate AChE^{28,51,52}. Previous review on acetylcholinesterase of *Caenorhabditis elegans* has reported that four AChEs perform non-overlapping functions and each has its own distinct patterns of expression in different organs⁵³. It suggests that during evolutionary events, functional differentiation also occurred in these distinct *ace* loci; and might also apply to these three *A. besseyi ace* genes.

The functions of three AbeAChEs were predicted by aligning the amino acid sequences with *Torpedo californica* AChE whose functional domains had been well studied. The alignment indicates that RI and HSF shared similar AChEs and had the same sequences in the catalytic regions with TcAChE (Fig. 4). Thus, we inferred that AChEs of the two isolates had similar affinities not only to acetylcholine but also to AChE-inhibitors. However, whether the amino acids differences of RI and HSF AChEs in non-functional parts might contribute to their sensibilities to AChE inhibitors still remains unknown. Molecular docking was performed to predict the affinities of AChEs to fenamiphos. The results suggested that each AChE of RI isolate had lower affinities to fenamiphos than AChEs of HSF isolate, especially AChE1 and AChE3 proteins, which correlates the lower sensitivity of RI isolate to the fenamiphos. However, the further protein-level experiments will be needed to conclude the predicted differences in hydrogen bonds. The results could lead to the difference of fenamiphos sensitivities between two isolates.

For the non-catalytic subunits of the AChEs in the two isolates, both AbeAChE1/2 had a signal peptide and a transmembrane domain at N-terminus. AbeAChE3 had a transmembrane domain at C-terminus, and only AbeAChE2 had a GPI-anchor at C-terminus. The characteristics of AChEs non-catalytic subunits of *A. besseyi* are not found in those of four reference nematodes *C. elegans*, *M. incognita*, *B. xylophilus* and *Ditylenchus destructor*. However, the phylogenetic analysis clearly predicts the functions of the three AbeAChEs found in this study based on the sequence similarity^{28,34,53,54}. By comparing with *ace* genes sequence data of other nematodes, we could predict their function and expression sites. We speculated that AbeAChE1/2 might locate in neural network and muscle cells, and play non-overlapping roles in

synaptic transmission and early development. The AbeAChE3 might participate in non-neuronal functions, such as xenobiotic substances defense.

Comparing the basal expression levels of *ace* genes in two *A. besseyi* isolates, fenamiphos-susceptible HSF isolate was higher than RI isolate in all three *ace* genes. In human and mice AChE studies, high basal expression level of AChE led to hypersensitivity to AChE-inhibitors and failed to transcriptionally induce AChE production when exposure to AChE-inhibitors⁵⁵. The phenomenon was similar to the qRT-PCR results (Fig. 6) observed in these two *A. besseyi* isolates. Fenamiphos-sensitive HSF isolate displays a higher expression level of three *ace* genes. However, whether the basal expression level of *ace* genes directly influences AChE-inhibitor sensitivity in *A. besseyi* needs further experiments to be confirmed. To explore the reasons of different basal expression levels in these two *A. besseyi* isolates, the 5' flanking regions (6000 base-pairs) of the three *ace* genes in unpublished genome database were searched but no published promoter sequences^{55–59} of AChE were matched in these regions. The 5' flanking regions of each *ace* genes in two isolates only shared 85–89% identity. Whether the differences are associated with *ace* genes expression levels could not be concluded at this point.

Three *ace* genes of RI isolate were up-regulated after 100 ppm fenamiphos treatment. In a mice study, higher *ace* gene expression level was observed when mice were stressed with an AChE-inhibitor. The authors speculate that transcription factor c-Fos was triggered by an AChE-inhibitor, which affects the activities of the genes involved in acetylcholine metabolism, and leads to the different acetylcholinesterase expression level⁶⁰. Studies in greenbug (*Schizaphis graminum*) also found that increasing expression of AChE will lead to increased AChE activity and resistance to organophosphate²⁴. Furthermore, *ace* genes duplication, which was proportional to levels of transcript would lead to up-regulation of *ace* genes and result in organophosphate resistance^{21,23,26}. Based on the unpublished genome data, *A. besseyi* RI isolate has only one copy of each *ace* gene. Up-regulation of all three AChEs in RI might explain why R1 isolate is less sensitive to fenamiphos. By contrast, HSF isolate, which is susceptible to fenamiphos showed down-regulation of *ace* genes after fenamiphos treatment. Thought the organophosphate was considered as an AChE-inhibitor that cannot mediate *ace* genes expression⁵⁹, our results suggested that *ace* genes expression levels in *A. besseyi* was associate with the exposure to fenamiphos. In a study on human neuronal acetylcholinesterase expression, a chemical dioxin was found to down-regulate *ace* gene expression in human neuroblastoma cells transcriptionally or post-transcriptionally via the aryl hydrocarbon receptor (AhR) pathway or other mechanisms^{59,61}. It indicated that *ace* genes regulation is an intricate process, and we speculate that organophosphate might contribute to this complex pathway.

Instead of regulation of neuronal *ace* genes, some reports in arthropod and nematodes showed that production of non-neuronal acetylcholinesterase provides tolerance to xenobiotics, such as pesticides^{21,29,30,62}. For example, knocking down *ace-3* in *B. xylophilus* significantly increased their sensitivity to organophosphates and carbamates because *Bxace-3* provides the non-neuronal function of chemical defense²⁹. The phenomenon was observed in *C. elegans* as well, and it reveals that up-

regulation of *ace-3* could result in the detoxification of organophosphate³⁰. In our case, up-regulation of *ace-3* was also observed in fenamiphos-treated RI isolate, and might also contribute to the low sensitivity to fenamiphos in RI isolate.

In summary, two *A. besseyi* isolates, RI and HSF, showed different susceptibilities to organophosphate nematicide fenamiphos. By studying the three *ace* gene sequences and expressing regulation of these two isolates, we speculate that the different susceptibilities to fenamiphos in two isolates might be due to the point mutations responsible for different hydronic bond affinities and hydronic bond numbers, and the *ace* genes regulation. Low affinity and up-regulation of both neuronal and non-neuronal *ace* genes in RI isolate might be responsible to the lower sensitivity to fenamiphos, but the mechanisms of gene regulation are still unknown. Besides, because *ace* genes were down-regulated by fenamiphos in the high-susceptible isolate HSF, we reason that fenamiphos can block the activity of AChE and also contribute to the regulation of *ace* genes expression.

Declarations

Acknowledgements

The authors would like to thank Dr. Isheng Jason Tsai for sharing the unpublished *Aphelenchoides besseyi* genomic data, and Dr. Chia-Ching Chu for the technical support of qPCR.

References

1. Lilley, C. J., Kyndt, T. & Gheysen, G. Nematode Resistant GM Crops in Industrialised and Developing Countries. in *Genomics and Molecular Genetics of Plant-Nematode Interactions* 517–541 (Springer, 2011). doi:10.1007/978-94-007-0434-3_24
2. G., R.V., Webster, R. K. & Gunnell, P. S. *Compendium of Rice Diseases. Mycologia* **84**, (The American Phytopathological Society (APS), 1992).
3. Wu, H.-Y. The Occurrence of White Tip of Rice in the Northern Part of Taiwan and Improvement of Rice Seed Treatment Method. *Bull. Taoyuan Dist. Agric. Res. Ext. Stn.* **70**, 51–60 (2011).
4. Kyndt, T., Fernandez, D. & Gheysen, G. Plant-Parasitic Nematode Infections in Rice: Molecular and Cellular Insights. *Annu. Rev. Phytopathol.* **52**, 135–153 (2014).
5. Jones, J. T. *et al.* Top 10 plant-parasitic nematodes in molecular plant pathology. *Mol. Plant Pathol.* **14**, 946–961 (2013).
6. Youssef, M. M. A. The Leaf and Bud Nematode, *Aphelenchoides besseyi*, its Identification, Economic Importance and Control Measures. A Review. *Middle East J. Res.* **3**, 461–464 (2014).
7. Kang, J. S., Moon, Y. S. & Lee, S. H. Inhibition properties of three acetylcholinesterases of the pinewood nematode *Bursaphelenchus xylophilus* by organophosphates and carbamates. *Pestic. Biochem. Physiol.* **104**, 157–162 (2012).

8. Colovic, M. B., Krstic, D. Z., Lazarevic-Pasti, T. D., Bondzic, A. M. & Vasic, V. M. Acetylcholinesterase Inhibitors: Pharmacology and Toxicology. *Curr. Neuropharmacol.* **11**, 315–335 (2013).
9. Casida, J. E. & Durkin, K. A. Neuroactive Insecticides: Targets, Selectivity, Resistance, and Secondary Effects. *Annu. Rev. Entomol.* **58**, 99–117 (2013).
10. Hoshino, S. & Togashi, K. Effect of water-soaking and air-drying on survival of *Aphelenchoides besseyi* in *Oryza sativa* seeds. *J. Nematol.* **32**, 303–308 (2000).
11. Sparks, T. C. & Nauen, R. IRAC: Mode of action classification and insecticide resistance management. *Pestic. Biochem. Physiol.* **121**, 122–128 (2015).
12. Naqqash, M. N., Gökçe, A., Bakhsh, A. & Salim, M. Insecticide resistance and its molecular basis in urban insect pests. *Parasitol. Res.* **115**, 1363–1373 (2016).
13. Montella, I. R., Schama, R. & Valle, D. The classification of esterases: An important gene family involved in insecticide resistance - A review. *Mem. Inst. Oswaldo Cruz* **107**, 437–449 (2012).
14. Kliot, A. & Ghanim, M. Fitness costs associated with insecticide resistance. *Pest Manag. Sci.* **68**, 1431–1437 (2012).
15. Hotelier, T., Nègre, V., Marchot, P. & Chatonnet, A. Insecticide resistance through mutations in cholinesterases or carboxylesterases: Data mining in the ESTHER database. *J. Pestic. Sci.* **35**, 315–320 (2010).
16. Elanga-Ndille, E. *et al.* The g119s acetylcholinesterase (Ace-1) target site mutation confers carbamate resistance in the major malaria vector *Anopheles gambiae* from cameroon: A challenge for the coming irs implementation. *Genes (Basel)*. **10**, 1–14 (2019).
17. Yang, C., Feng, X., Liu, N., Li, M. & Qiu, X. Target-site mutations (AChE-G119S and kdr) in Guangxi *Anopheles sinensis* populations along the China-Vietnam border. *Parasites and Vectors* **12**, 1–7 (2019).
18. Keïta, M. *et al.* Acetylcholinesterase (ace-1R) target site mutation G119S and resistance to carbamates in *Anopheles gambiae* (sensu lato) populations from Mali. *Parasit. Vectors* **13**, 1–9 (2020).
19. Kotze, A. C. & Prichard, R. K. Anthelmintic Resistance in *Haemonchus contortus*. History, Mechanisms and Diagnosis. in *Advances in Parasitology* **93**, 397–428 (Elsevier, 2016).
20. Huang, W. K. *et al.* Mutations in Acetylcholinesterase2 (ace2) increase the insensitivity of acetylcholinesterase to fosthiazate in the root-knot nematode *Meloidogyne incognita*. *Sci. Rep.* **6**, 1–9 (2016).
21. Lee, S. H., Kim, Y. H., Kwon, D. H., Cha, D. J. & Kim, J. H. Mutation and duplication of arthropod acetylcholinesterase: Implications for pesticide resistance and tolerance. *Pestic. Biochem. Physiol.* **120**, 118–124 (2015).
22. Charpentier, A. & Fournier, D. Levels of total acetylcholinesterase in *Drosophila melanogaster* in relation to insecticide resistance. *Pestic. Biochem. Physiol.* **70**, 100–107 (2001).

23. Berrada, S. &Fournier, D. Transposition-mediated transcriptional overexpression as a mechanism of insecticide resistance. *Mol. Gen. Genet.* **256**, 348–354 (1997).
24. Gao, J. R. &Zhu, K. Y. Increased expression of an acetylcholinesterase gene may confer organophosphate resistance in the greenbug, *Schizaphis graminum* (Homoptera: Aphididae). *Pestic. Biochem. Physiol.* **73**, 164–173 (2002).
25. Kwon, D. H., Choi, J. Y., Je, Y. H. &Lee, S. H. The overexpression of acetylcholinesterase compensates for the reduced catalytic activity caused by resistance-conferring mutations in *Tetranychus urticae*. *Insect Biochem. Mol. Biol.* **42**, 212–219 (2012).
26. Kwon, D. H., Clarkt, J. M. &Lee, S. H. Extensive gene duplication of acetylcholinesterase associated with organophosphate resistance in the two-spotted spider mite. *Insect Molecular Biology* **19**, 195–204 (2010).
27. Jameson, R. R., Seidler, F. J. &Slotkin, T. A. Nonenzymatic functions of acetylcholinesterase splice variants in the developmental neurotoxicity of organophosphates: Chlorpyrifos, chlorpyrifos oxon, and diazinon. *Environ. Health Perspect.* **115**, 65–70 (2007).
28. Kim, Y. H. &Lee, S. H. Invertebrate acetylcholinesterases: Insights into their evolution and non-classical functions. *J. Asia. Pac. Entomol.* **21**, 186–195 (2018).
29. Kang, J. S., Lee, D. W., Koh, Y. H. &Lee, S. H. A soluble acetylcholinesterase provides chemical defense against xenobiotics in the pinewood nematode. *PLoS One* **6**, 1–7 (2011).
30. Han, Y., Song, S., Guo, Y., Zhang, J. &Ma, E. ace-3 plays an important role in phoxim resistance in *Caenorhabditis elegans*. *Ecotoxicology* **25**, 835–844 (2016).
31. Jen, F. Y., Tsay, T. T. &Chen, P. *Aphelenchoides bicaudatus* from ornamental nurseries in Taiwan and its relationship with some agricultural crops. *Plant Dis.* **96**, 1763–1766 (2012).
32. Hsieh, S. H., Lin, C. J. &Chen, P. Sexual compatibility among different host-originated isolates of *Aphelenchoides besseyi* and the inheritance of the parasitism. *PLoS One* **7**, (2012).
33. Ritz, C., Baty, F., Streibig, J. C. &Gerhard, D. Dose-response analysis using R. *PLoS One* **10**, 1–13 (2015).
34. Kang, J. S. *et al.* Three acetylcholinesterases of the pinewood nematode, *Bursaphelenchus xylophilus*: Insights into distinct physiological functions. *Mol. Biochem. Parasitol.* **175**, 154–161 (2011).
35. Kumar, S., Stecher, G. &Tamura, K. MEGA7: Molecular Evolutionary Genetics Analysis Version 7.0 for Bigger Datasets. *Mol. Biol. Evol.* **33**, 1870–1874 (2016).
36. Le, S. Q. &Gascuel, O. An improved general amino acid replacement matrix. *Mol. Biol. Evol.* **25**, 1307–1320 (2008).
37. Felsenstein, J. Confidence Limits on Phylogenies: An Approach Using the Bootstrap. *Evolution (N. Y.)* **39**, 783 (1985).
38. Carlier, P. R. *et al.* Towards a species-selective acetylcholinesterase inhibitor to control the mosquito vector of malaria, *Anopheles gambiae*. *Chem. Biol. Interact.* **175**, 368–375 (2008).

39. Möller, S., Croning, M. D. R. &Apweiler, R. Evaluation of methods for the prediction of membrane spanning regions. *Bioinformatics* **17**, 646–653 (2001).
40. Almagro Armenteros, J. J. *et al.* SignalP 5.0 improves signal peptide predictions using deep neural networks. *Nat. Biotechnol.* **37**, 420–423 (2019).
41. Nielsen, H., Engelbrecht, J., Brunak, S. &vonHeijne, G. A neural network method for identification of prokaryotic and eukaryotic signal peptides and prediction of their cleavage sites. *Int. J. Neural Syst.* **8**, 581–599 (1997).
42. Pierleoni, A., Martelli, P. &Casadio, R. PredGPI: A GPI-anchor predictor. *BMC Bioinformatics* **9**, 1–11 (2008).
43. Yang, J. *et al.* The I-TASSER Suite: protein structure and function prediction. *Nat. Methods* **12**, 7–8 (2015).
44. Dassault Systèmes BIOVIA. Discovery Studio Modeling Environment, Release 2017. (2017).
45. Raves, M. L. *et al.* Structure of acetylcholinesterase complexed with the nootropic alkaloid,(-)-huperzine A. *Nat. Struct. Biol.* **4**, 57–63 (1997).
46. Wu, G., Robertson, D. H., Brooks III, C. L. &Vieth, M. Detailed analysis of grid-based molecular docking: A case study of CDOCKER—A CHARMM-based MD docking algorithm. *J. Comput. Chem.* **24**, 1549–1562 (2003).
47. Brooks, B. R. *et al.* CHARMM: a program for macromolecular energy, minimization, and dynamics calculations. *J. Comput. Chem.* **4**, 187–217 (1983).
48. Laskowski, R. A. &Swindells, M. B. LigPlot+: multiple ligand–protein interaction diagrams for drug discovery. (2011).
49. Wu, G. L., Kuo, T. H., Tsay, T. T., Tsai, I. J. &Chen, P. J. Glycoside hydrolase (gh) 45 and 5 candidate cellulases in aphelenchoides besseyei isolated from bird's-nest fern. *PLoS One* **11**, 1–17 (2016).
50. Whittaker, J. H., Carlson, S. A., Jones, D. E. &Brewer, M. T. Molecular mechanisms for anthelmintic resistance in strongyle nematode parasites of veterinary importance. *J. Vet. Pharmacol. Ther.* **40**, 105–115 (2017).
51. Pezzementi, L. &Chatonnet, A. Evolution of cholinesterases in the animal kingdom. *Chem. Biol. Interact.* **187**, 27–33 (2010).
52. Cha, D. J. &Lee, S. H. Evolutionary origin and status of two insect acetylcholinesterases and their structural conservation and differentiation. *Evol. Dev.* **17**, 109–119 (2015).
53. Selkirk, M. E., Lazari, O., Hussein, A. S. &Matthews, J. B. Nematode acetylcholinesterases are encoded by multiple genes and perform non-overlapping functions. *Chem. Biol. Interact.* **157–158**, 263–268 (2005).
54. Cui, R. *et al.* Expression and evolutionary analyses of three acetylcholinesterase genes (Mi-ace-1, Mi-ace-2, Mi-ace-3) in the root-knot nematode Meloidogyne incognita. *Exp. Parasitol.* **176**, 75–81 (2017).
55. Shapira, M. A transcription-activating polymorphism in the ACHE promoter associated with acute sensitivity to anti-acetylcholinesterases. *Hum. Mol. Genet.* **9**, 1273–1281 (2000).

56. Zhang, J. Y. *et al.* The JNK/AP1/ATF2 pathway is involved in H₂O₂-induced acetylcholinesterase expression during apoptosis. *Cell. Mol. Life Sci.* **65**, 1435–1445 (2008).
57. Deng, R. *et al.* Acetylcholinesterase expression mediated by c-Jun-NH₂-terminal kinase pathway during anticancer drug-induced apoptosis. *Oncogene* **25**, 7070–7077 (2006).
58. Culetto, E. *et al.* Structure and promoter activity of the 5' flanking region of ace-1, the gene encoding acetylcholinesterase of class A in *Caenorhabditis elegans*. *J. Mol. Biol.* **290**, 951–966 (1999).
59. Xie, H. Q. *et al.* AhR-mediated effects of dioxin on neuronal acetylcholinesterase expression in vitro. *Environ. Health Perspect.* **121**, 613–618 (2013).
60. Kaufer, D., Friedman, A., Seidman, S. & Soreq, H. Acute stress facilitates long-lasting changes in cholinergic gene expression. *Nature* **393**, 373–377 (1998).
61. Xie, H. Q. *et al.* New perspectives for multi-level regulations of neuronal acetylcholinesterase by dioxins. *Chem. Biol. Interact.* **259**, 286–290 (2016).
62. Kim, Y. H., Kwon, D. H., Ahn, H. M., Koh, Y. H. & Lee, S. H. Induction of soluble AChE expression via alternative splicing by chemical stress in *Drosophila melanogaster*. *Insect Biochem. Mol. Biol.* **48**, 75–82 (2014).

Figures

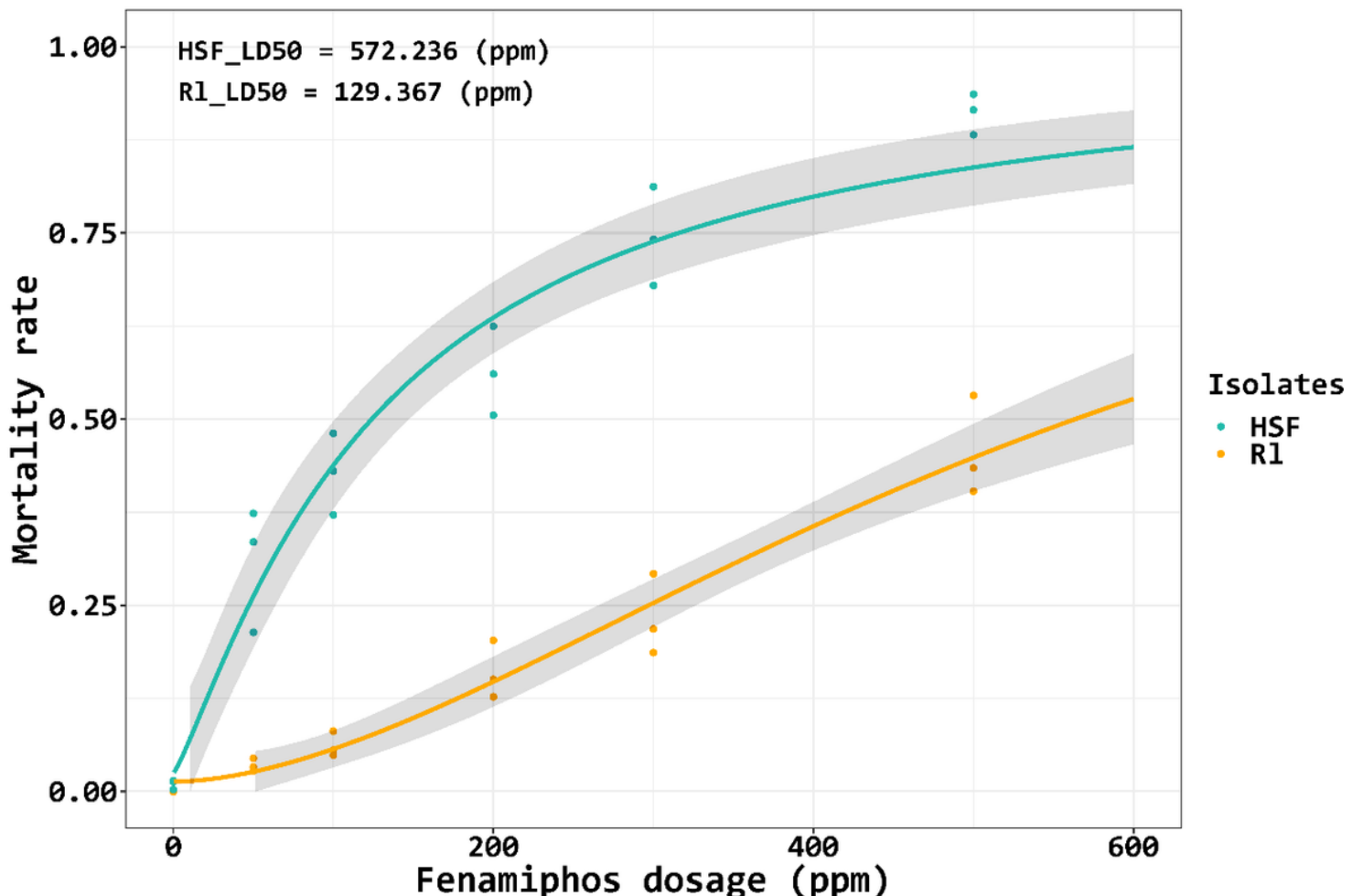


Figure 1

The fenamiphos dose-response curves correlating to the mortality rates of *Aphelenchoides besseyi* RI and HSF isolates. Each point represents the mortality rate of population treated with corresponding fenamiphos dosage in one replicate. Confidence bands were presented by a grey band. The median lethal doses (LD50) of two isolates to fenamiphos were displayed at the top-left of the figure.

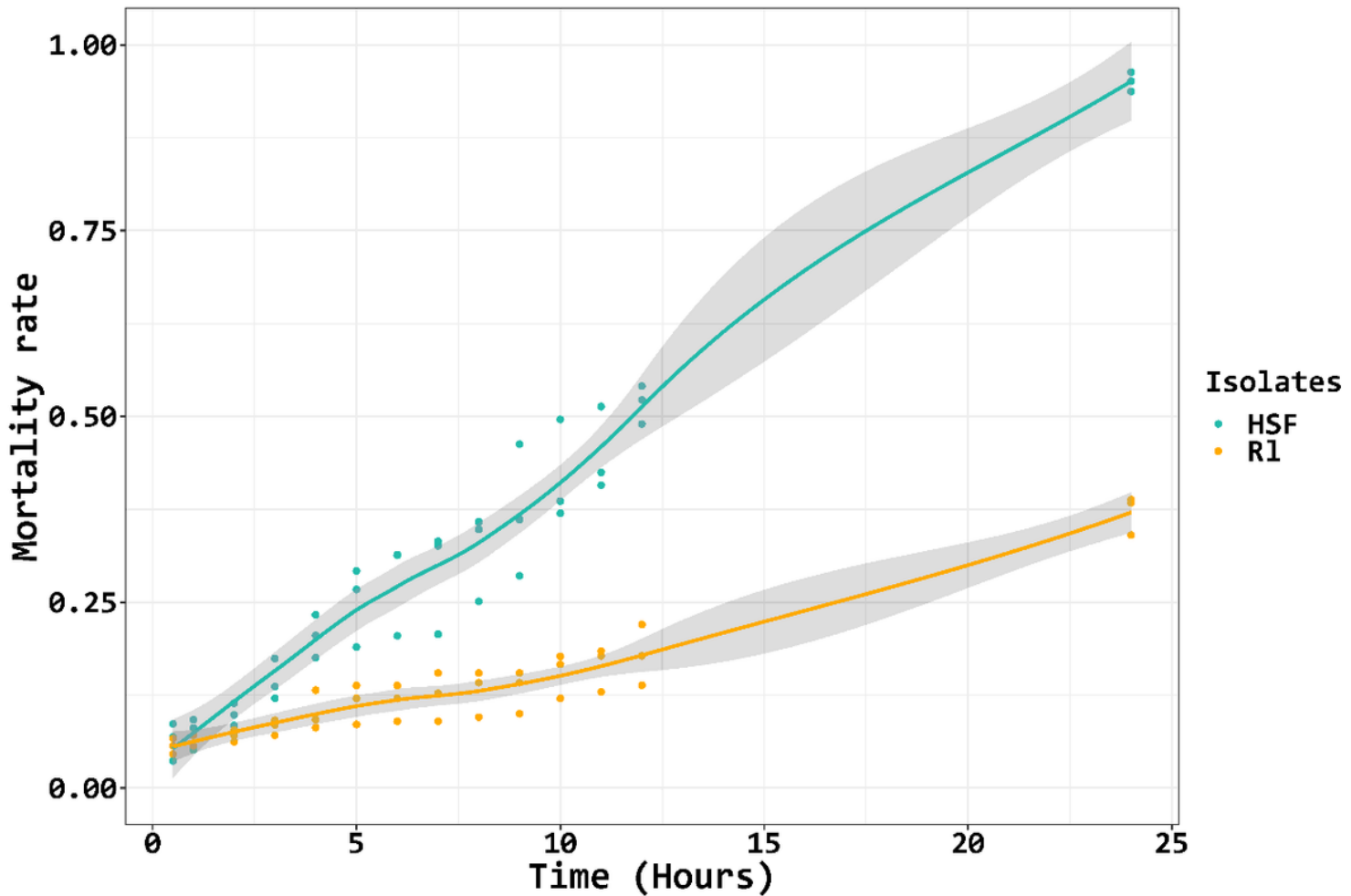


Figure 2

A maximum likelihood phylogeny of six AbeAChEs with the AChEs and BuChEs from Vertebrata, Arthropoda and Nematoda. The phylogenetic tree was generated using a ClustalW alignment and maximum likelihood tree with 500 bootstrap replicates. The GenBank accession numbers of each gene are indicated in parentheses. The six AbeAChEs are indicated by bold and red font.

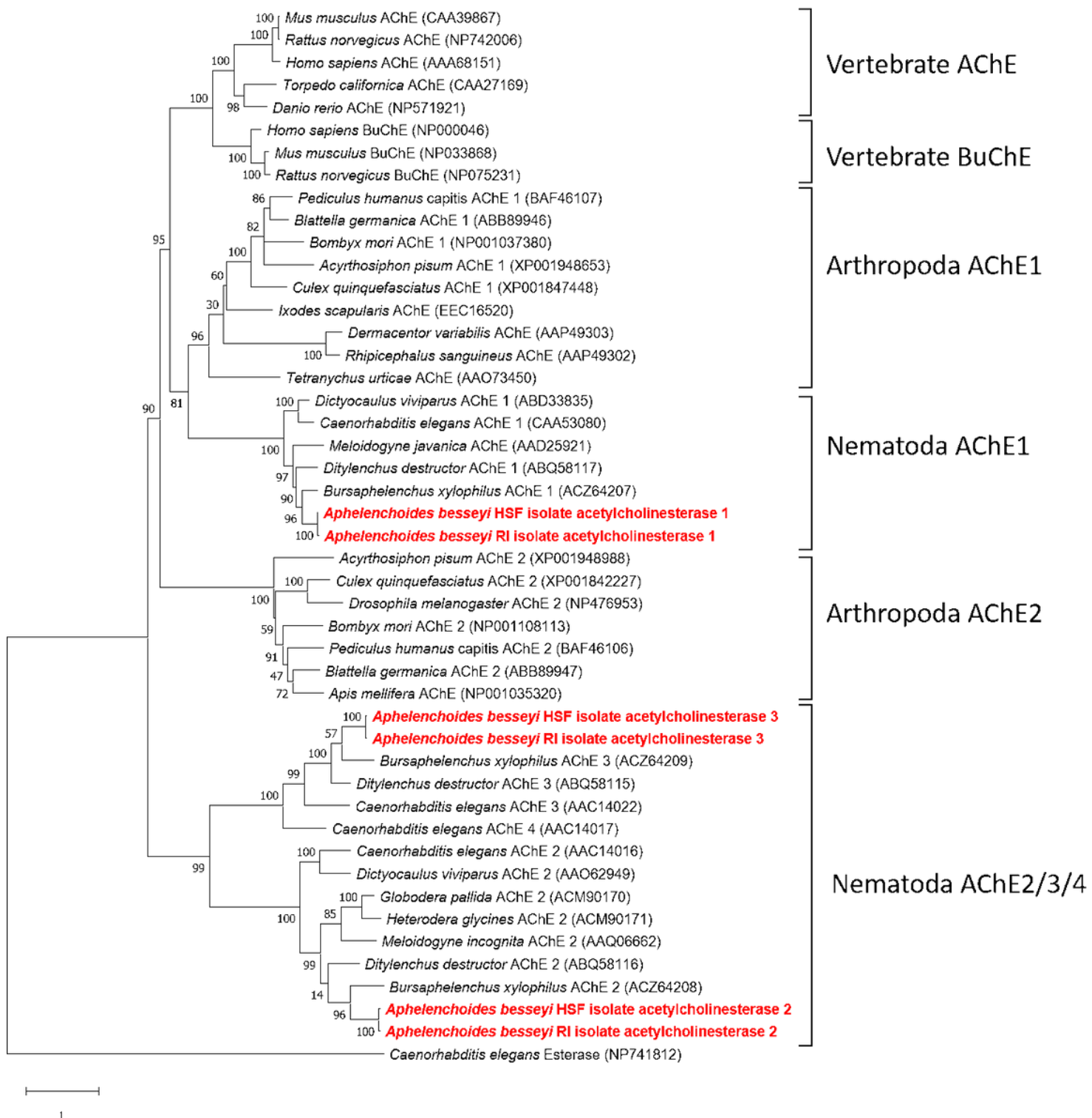


Figure 3

A maximum likelihood phylogeny of six AbeAChEs with the AChEs and BuChEs from Vertebrata, Arthropoda and Nematoda. The phylogenetic tree was generated using a ClustalW alignment and maximum likelihood tree with 500 bootstrap replicates. The GenBank accession numbers of each gene are indicated in parentheses. The six AbeAChEs are indicated by bold and red font.

	Catalytic triad			Oxyanion hole			Choline-binding site	
TcAChE	200 TIFGE S AGGAS	327 E	440 H	116 YGG F	201 A		84 W	330 FF
R1_AChE1	218 TLFGE S AGAAS	350 E	472 H	135 YGG F	219 A		101 W	353 YF
HSF_AChE1	219 TLFGE S AGAAS	351 E	473 H	136 YGG F	220 A		102 W	354 YF
R1_AChE2	226 TLFGE S AGGAS	362 E	490 H	143 FG GGF	227 A		113 W	365 YW
HSF_AChE2	228 TLFGE S AGGAS	364 E	492 H	145 FG GGF	229 A		115 W	367 YW
R1_AChE3	224 SLFGE S AGASS	352 E	469 H	141 FG GGF	225 A		109 W	355 FW
HSF_AChE3	224 SLFGE S AGASS	352 E	469 H	141 FG GGF	225 A		109 W	355 FW
	Acyl pocket			Peripheral site			Flexible peripheral site loop	
TcAChE	233 W	288 F	290 F	70 Y	72 D	121 Y	279 W	334 YG
R1_AChE1	251 W	311 A	313 F	87 S	89 D	140 W	304 W	357 YQ
HSF_AChE1	252 W	312 A	314 F	88 S	90 D	141 W	305 W	358 YQ
R1_AChE2	259 W	321 M	323 F	99 S	101 D	148 F	311 D	369 YY
HSF_AChE2	261 W	323 M	325 F	101 S	103 D	150 F	311 D	371 YY
R1_AChE3	257 W	312 F	314 F	95 P	97 D	146 Y	303 W	359 YN
HSF_AChE3	257 W	312 F	314 F	95 P	97 D	146 Y	303 W	359 YN

Figure 4

Alignment of *Torpedo californica* and *Aphelenchoides besseyi* AChEs. Residues marked in red and bold font are essential for catalysis. Numbering of AbeAChEs is based on the protein sequences that translated from the coding sequences.

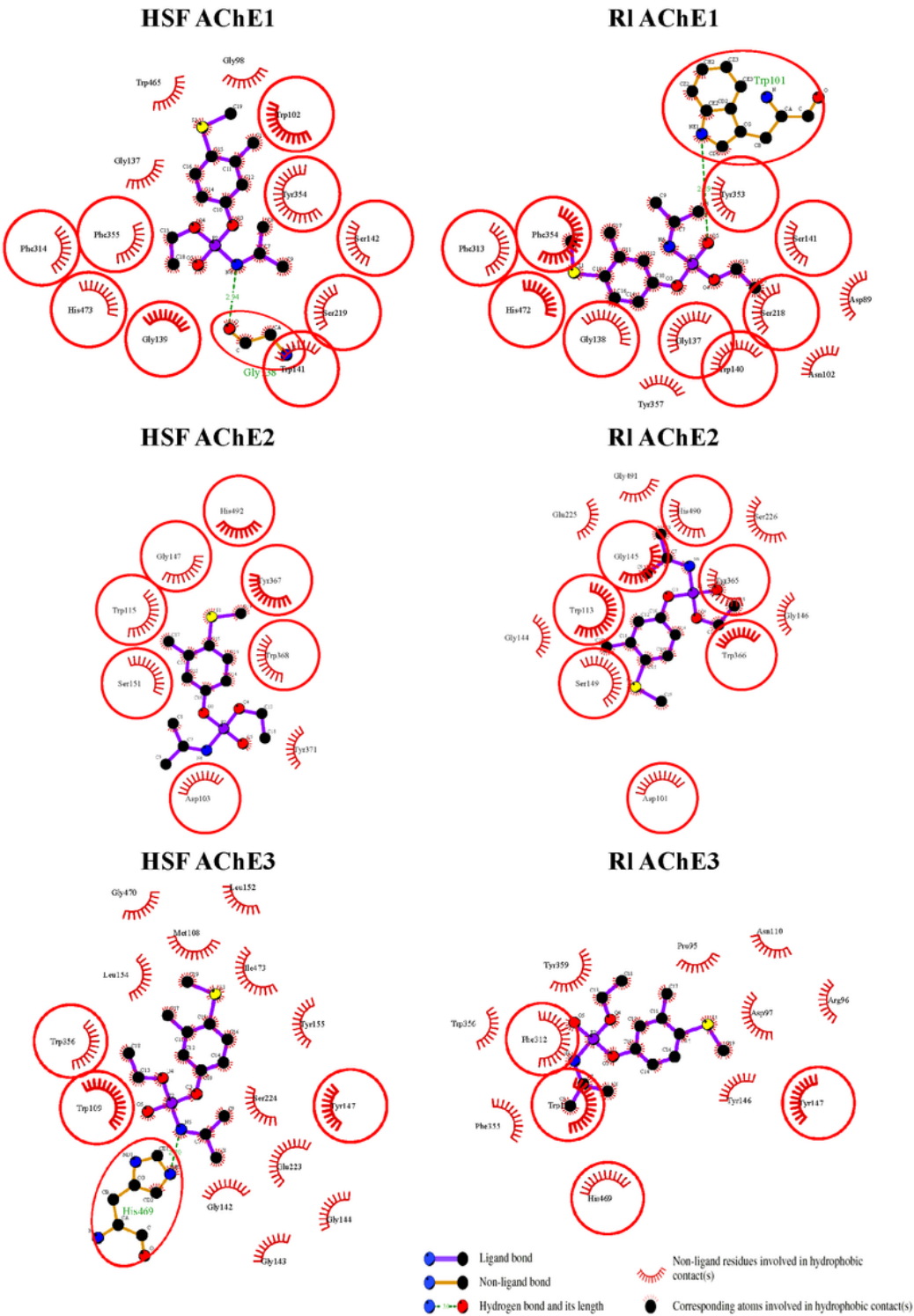


Figure 5

Schematic of the interaction between fenamiphos and AChE-residues. The key residues surrounding the acetylcholine-binding pocket of AChE1, AChE2, and AChE3 proteins were identified via the best docking poses. The red circles and ellipses indicate the identical residues in both HSF and RI isolates.

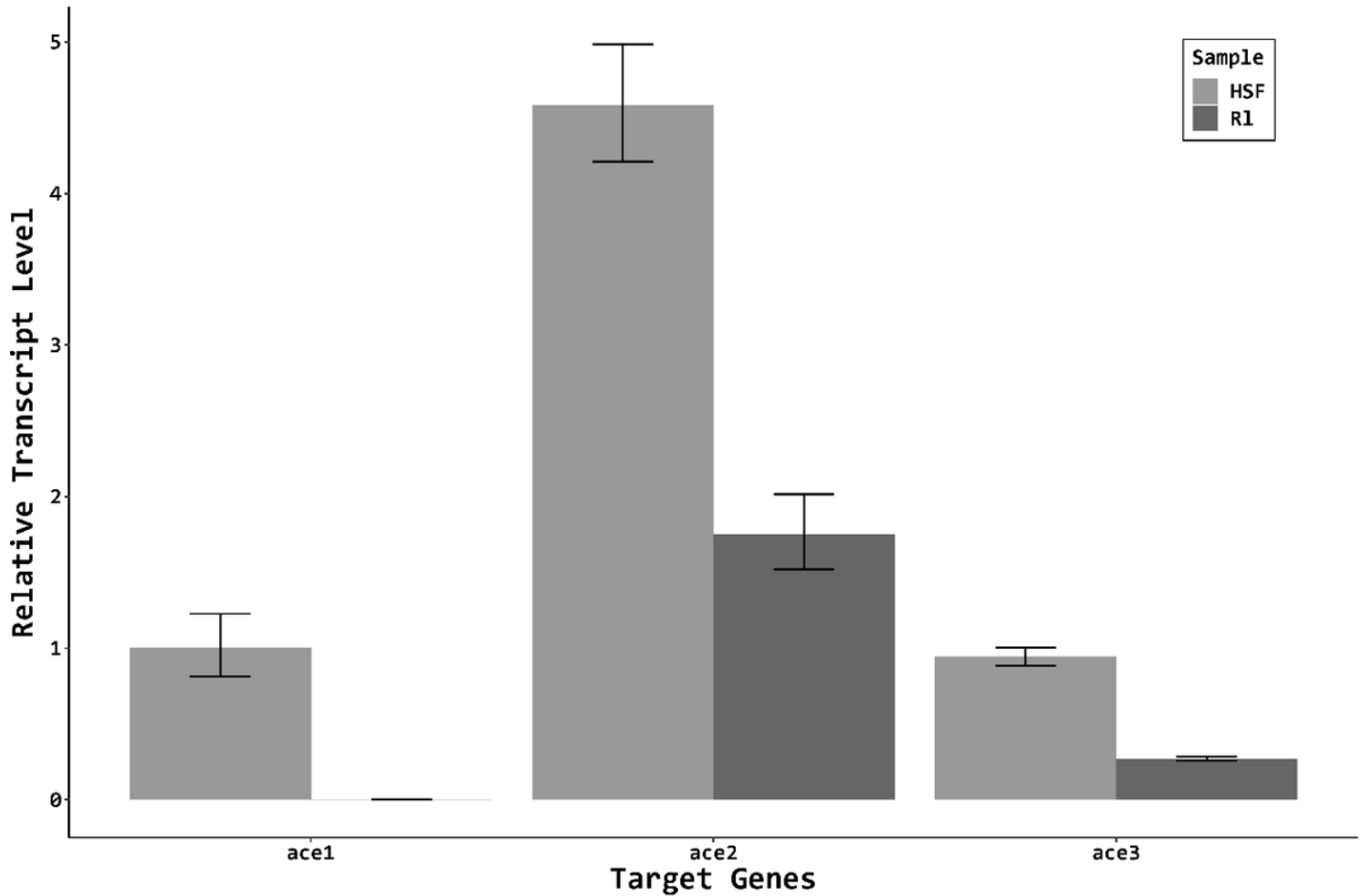


Figure 6

The relative transcript level of the three ace genes compared to a reference gene (18s) in the two *Aphelenchoides besseyi* isolates normalized to the HSF AChE1 gene. Error bars represent standard errors. The experiments were performed with three biological replicates, each having three technical replicates.

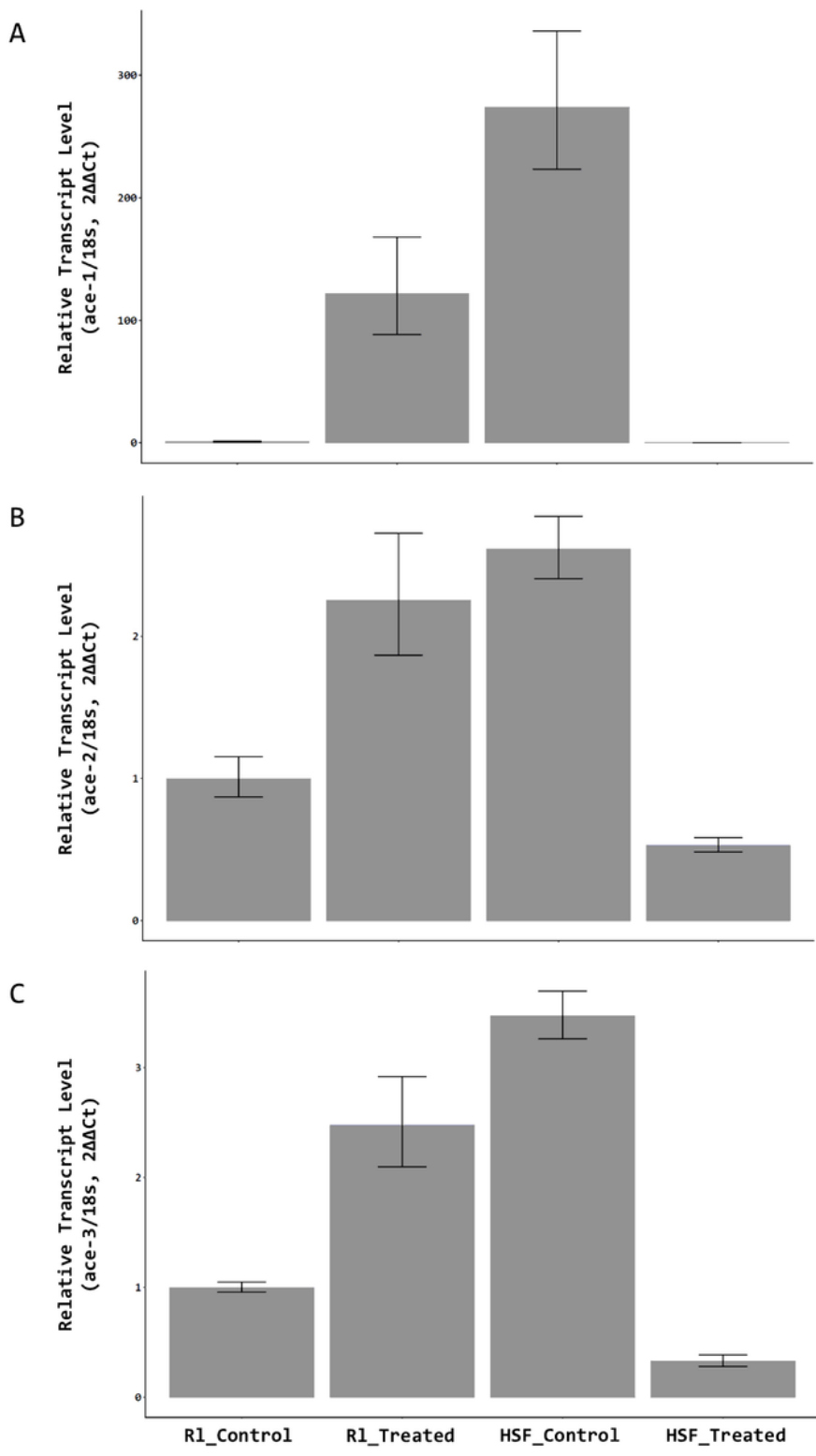


Figure 7

Effect of 12-hour-treatments of 100 ppm fenamiphos on transcript abundance of three ace genes in two *Aphelenchoides besseyi* isolates, transcription levels were normalized to R1 control treatments. Error bars represent standard errors. The experiments were performed with three biological replicates, each having three technical replicates.

Supplementary Files

This is a list of supplementary files associated with this preprint. Click to download.

- [SupplementTableS1.docx](#)